BUKTI

SUBMIT

MANUSKRIP

PENULIS MERUPAKAN PENULIS PERTAMA DAN SELALU BERKOMUNIKASI DENGAN KOREPONDING AUTHOR SELAMA PROSES PUBLIKASI, SEBAGAIMANA TERLAMPIR

Universitas Hasanuddin

Andi Dian Permana <andi.dian.permana@farmasi.unhas.ac.id>

Fwd: Confirm co-authorship of submission to European Journal of Pharmaceutics and Biopharmaceutics

1 message

Andi Permana <apermana01@qub.ac.uk> Tue, Apr 4, 2023 at 4:20 PM
To: Andi Dian Permana <andi.dian.permana@farmasi.unhas.ac.id>

Get Outlook for iOS

From: em.ejpb.0.6aad06.3a58b133@editorialmanager.com <em.ejpb.0.6aad06.3a58b133@editorialmanager.com> on behalf of European Journal of Pharmaceutics and Biopharmaceutics <em@editorialmanager.com>
Sent: Friday, April 17, 2020 7:59:44 PM
To: Andi Permana <apermana01@qub.ac.uk>
Subject: Confirm co-authorship of submission to European Journal of Pharmaceutics and Biopharmaceutics

This message is from an external sender. Please take care when responding, clicking links or opening attachments.

This is an automated message.

Dissolving Microneedle-Mediated Dermal Delivery of Itraconazole Nanocrystals for Improved Treatment of Cutaneous Candidiasis by Professor Ryan Donnelly

Dear Permana,

You have been listed as a contributing author for the above referenced manuscript. Please confirm whether you are a contributing author by clicking one of the following links.

Yes, I made a significant contribution to this manuscript and meet the criteria for authorship (detailed in the Guide for Authors of European Journal of Pharmaceutics and Biopharmaceutics)

https://www.editorialmanager.com/ejpb/l.asp?i=70952&l=6MDFXAEE . You may be asked to register to complete this confirmation. Once complete, you will be able to view the status of the submission as it goes through the editorial process by logging in at https://www.editorialmanager.com/ejpb/.

No, I did not contribute significantly to this manuscript and do not meet the criteria for authorship: https://www.editorialmanager.com/ejpb/l.asp?i=70953&l=IY18B0Y7.

If, for any reason, the above links do not work, please log in as an author at https://www.editorialmanager.com/ejpb/.

Thank you in advance for your confirmation.

Kind regards,
European Journal of Pharmaceutics and Biopharmaceutics

More information and support

FAQ: What is Editorial Manager Co-Author registration?
https://service.elsevier.com/app/answers/detail/a_id/28460/supporthub/publishing/kw/co-author+editorial+manager/

You will find information relevant for you as an author on Elsevier's Author Hub: https://www.elsevier.com/authors.

FAQ: How can I reset a forgotten password?
https://service.elsevier.com/app/answers/detail/a_id/28452/supporthub/publishing/kw/editorial+manager/

For further assistance, please visit our customer service site: https://service.elsevier.com/app/home/supporthub/publishing/. Here you can search for solutions on a range of topics, find answers to frequently asked questions, and learn more about Editorial Manager via interactive tutorials. You can also talk 24/7 to our customer support team by phone and 24/7 by live chat and email.

In compliance with data protection regulations, you may request that we remove your personal registration details at any time. (Use the following URL: https://www.editorialmanager.com/ejpb/login.asp?a=r). Please contact the publication office if you have any questions.

BUKTI REVIEW DARI REVIEWERS

Universitas Hasanuddin

Andi Dian Permana <andi.dian.permana@farmasi.unhas.ac.id>

Fwd: Your Submission EJPB-D-20-00409

2 messages

Andi Permana <apermana01@qub.ac.uk> Tue, Apr 4, 2023 at 4:20 PM
To: Andi Dian Permana <andi.dian.permana@farmasi.unhas.ac.id>

Get Outlook for iOS

From: Ryan Donnelly <R.Donnelly@qub.ac.uk>
Sent: Monday, June 22, 2020 10:30:25 PM
To: Andi Permana <apermana01@qub.ac.uk>
Cc: Alejandro Paredes <A.Paredes@qub.ac.uk>
Subject: Fw: Your Submission EJPB-D-20-00409

Please see below Dian,

The comments should only take a matter of minutes, certainly less than an hour to address.

I'd like to get these resubmitted this week.

Are you able to do this?

If not, let me know and Alejandro and I can tackle this.

Very well done.

Ryan

Professor Ryan F. Donnelly
Chair in Pharmaceutical Technology
School of Pharmacy
Queen's University Belfast
Medical Biology Centre
97 Lisburn Road
Belfast
BT9 7BL
UK
Tel: +44 (0) 2890 972 251
Fax: +44 (0) 2890 247 794
Email: r.donnelly@qub.ac.uk

From: em.ejpb.0.6c20c6.d9cca4f0@editorialmanager.com <em.ejpb.0.6c20c6.d9cca4f0@editorialmanager.com> on behalf of European Journal of Pharmaceutics and Biopharmaceutics <em@editorialmanager.com>
Sent: 22 June 2020 15:08
To: Ryan Donnelly <R.Donnelly@qub.ac.uk>
Subject: Your Submission EJPB-D-20-00409

Ref.: Ms. No. EJPB-D-20-00409
Dissolving Microneedle-Mediated Dermal Delivery of Itraconazole Nanocrystals for Improved Treatment of Cutaneous Candidiasis
European Journal of Pharmaceutics and Biopharmaceutics

Dear Professor Donnelly,

Thank you for submitting your manuscript to European Journal of Pharmaceutics and Biopharmaceutics. I have received comments from reviewers on your manuscript. Your paper should become acceptable for publication pending suitable minor revision and modification of the article in light of the appended reviewer comments.

When resubmitting your manuscript, please carefully consider all issues mentioned in the reviewers' comments, outline every change made point by point, and provide suitable rebuttals for any comments not addressed.

To submit your revised manuscript go to https://www.editorialmanager.com/ejpb/ and log in as an Author where you will see a menu item called 'Submission Needing Revision'.

Please resubmit your manuscript by Aug 21, 2020.

I look forward to receiving your revised manuscript.

Yours sincerely

Thomas Rades
Editor
European Journal of Pharmaceutics and Biopharmaceutics

Comments from the Editors and Reviewers:
This detailed and comprehensive manuscript provides an interesting and detailed study focusing on a specific clinical outcome.

The manuscript is therefore narrow in its scope and an understanding of the broader application of this work would be useful to see as this study is similar in its core methods and structure to several others from this research group.

The issue of Ostwald ripening (citing reference 40) would be worth expanding particularly in the context of particle size range and the impact on device stability and performance.

*****

Data in Brief (optional):
We invite you to convert your supplementary data (or a part of it) into an additional journal publication in Data in Brief, a multi-disciplinary open access journal. Data in Brief articles are a fantastic way to describe supplementary data and associated metadata, or full raw datasets deposited in an external repository, which are otherwise unnoticed. A Data in Brief article (which will be reviewed, formatted, indexed, and given a DOI) will make your data easier to find, reproduce, and cite.

You can submit to Data in Brief via the journals submission system when you upload your revised manuscript. To do so, complete the template and follow the co-submission instructions found here: www.elsevier.com/dib-template. If your manuscript is accepted, your Data in Brief submission will automatically be transferred to Data in Brief for editorial review and publication.

Please note: an open access Article Publication Charge (APC) is payable by the author or research funder to cover the costs associated with publication in Data in Brief and ensure your data article is immediately and permanently free to access by all. For the current APC see: www.elsevier.com/journals/data-in-

brief/2352-3409/open-access-journal

Please contact the Data in Brief editorial office at dib-me@elsevier.com or visit the Data in Brief homepage (www.journals.elsevier.com/data-in-brief/) if you have questions or need further information.

*****

MethodsX (optional)

We invite you to submit a method article alongside your research article. This is an opportunity to get full credit for the time and money spent on developing research methods, and to increase the visibility and impact of your work. If your research article is accepted, we will contact you with instructions on the submission process for your method article to MethodsX. On receipt at MethodsX it will be editorially reviewed and, upon acceptance, published as a separate method article. Your articles will be linked on ScienceDirect.

Please prepare your paper using the MethodsX Guide for Authors: https://www.elsevier.com/journals/methodsx/2215-0161/guide-for-authors (and template available here: https://www.elsevier.com/MethodsX-template) Open access fees apply.

Have questions or need assistance?
For further assistance, please visit our customer service site: http://help.elsevier.com/app/answers/list/p/9435/. Here you can search for solutions on a range of topics, find answers to frequently asked questions, and learn more about Editorial Manager via interactive tutorials. You can also talk 24/5 to our customer support team by phone and 24/7 by live chat and email.

In compliance with data protection regulations, you may request that we remove your personal registration details at any time. (Use the following URL: https://www.editorialmanager.com/ejpb/login.asp?a=r). Please contact the publication office if you have any questions.

Andi Permana <apermana01@qub.ac.uk> Tue, Apr 4, 2023 at 4:21 PM
To: Andi Dian Permana <andi.dian.permana@farmasi.unhas.ac.id>

Get Outlook for iOS

From: Andi Permana <apermana01@qub.ac.uk>
Sent: Tuesday, June 23, 2020 11:24:27 AM
To: Ryan Donnelly <R.Donnelly@qub.ac.uk>
Cc: Alejandro Paredes <A.Paredes@qub.ac.uk>
Subject: Re: Your Submission EJPB-D-20-00409

Hi Ryan and Alejandro,

I have revised the manuscript. Please find attached the files required for the resubmission.

Thank you very much,

Best wishes,
Dian

From: Ryan Donnelly <R.Donnelly@qub.ac.uk>
Sent: 22 June 2020 15:30
[Quoted text hidden]

[Quoted text hidden]

3 attachments

EJPB_MN-Itraconazole Nanocrystal_Revised.docx
7944K

Letter to Editor_EJPB.docx
122K

Response To Reviewers_EJPB.docx
33K

BUKTI SUBMIT HASIL REVIEW

EJPB-D-20-00409

Dissolving Microneedle-Mediated Dermal Delivery of Itraconazole Nanocrystals for Improved Treatment of Cutaneous Candidiasis European Journal of Pharmaceutics and Biopharmaceutics

Response to Reviewers

We are very thankful to the expert reviewers for taking the time to kindly review our manuscript and provide helpful comments for improvement and clarification. We have made some changes to the manuscript as a result of these comments. We believe that the manuscript is now substantially improved. We have addressed each of the reviewers' comments in detail below. blue. In terms of revision, we have highlighted the changes in our manuscript in yellow.

Comments from the Editors and Reviewers:

This detailed and comprehensive manuscript provides an interesting and detailed study focusing on a specific clinical outcome.

The manuscript is therefore narrow in its scope and an understanding of the broader application of this work would be useful to see as this study is similar in its core methods and structure to several others from this research group.

Response

We thank the editors and reviewers for their positive comments. Following the reviewer's suggestion, we have now added the following statements in the revised manuscript:

"Based on the findings presented in this extensive study, it is shown that the combination approach of NC and dissolving MNs could enhance the penetrability of ITZ in *ex vivo* candidiasis infection models in porcine skin, suggested by the excellent dermatokinetic profiles of ITZ and the great fungal burden decreases. The overriding benefit of this combinatorial delivery system we have shown in this work, compared to cream dosage form and needle-free patches, lead to high residence time specific delivery in the infected skin which could hypothetically improve the efficiency of antifungal therapy in cutaneous

candidiasis infection. Based on from these favourable findings, *in vivo* studies must now be carried out in a suitable animal model." (Line 615)

The issue of Ostwald ripening (citing reference 40) would be worth expanding particularly in the context of particle size range and the impact on device stability and performance.

Response

Thank for the advise. Following this suggestion, we have added the follwing explanation in our revised manuscript:

"It is important to note that the instability of nanoformulations caused by Ostwald ripening only occurs in the liquid state. In order to achieve stable nanoformulations, the complete drying of the nanoparticles is necessary (Levit et al., 2018). Therefore, the incorporation of NCs into a dry and solid dosage form, dissolving MNs, could be beneficial to obtain stable NC formulations." (Line 339)

Levit, S.L., Stwodah, R.M., Tang, C., 2018. Rapid, room temperature nanoparticle drying and low-energy reconstitution via electrospinning. J. Pharm. Sci. 107, 807–813.

Dissolving Microneedle-Mediated Dermal Delivery of Itraconazole Nanocrystals for Improved Treatment of Cutaneous Candidiasis

Andi Dian Permana[1], Alejandro J. Paredes[2,3], Fabiana Volpe-Zanutto[2], Qonita Kurnia Anjani[2], Emilia Utomo[2], Ryan F. Donnelly[2*]

1. Department of Pharmaceutics, Faculty of Pharmacy, Hasanuddin University, Makassar, Indonesia

2. School of Pharmacy, Queen's University Belfast, Medical Biology Centre, 97 Lisburn Road, Belfast. BT9 7BL, UK

3. Unidad de Investigación y Desarrollo en Tecnología Farmacéutica (UNITEFA) – CONICET, Córdoba, Argentina.

***Corresponding author:**
Professor Ryan F. Donnelly
Chair in Pharmaceutical Technology
School of Pharmacy
Queens University Belfast
Medical Biology Centre
97 Lisburn Road
Belfast
BT9 7BL, Northern Ireland
United Kingdom
Tel: +44 (0) 28 90 972 251
Fax: +44 (0) 28 90 247 794
Email: r.donnelly@qub.ac.uk

GRAPHICAL ABSTRACT

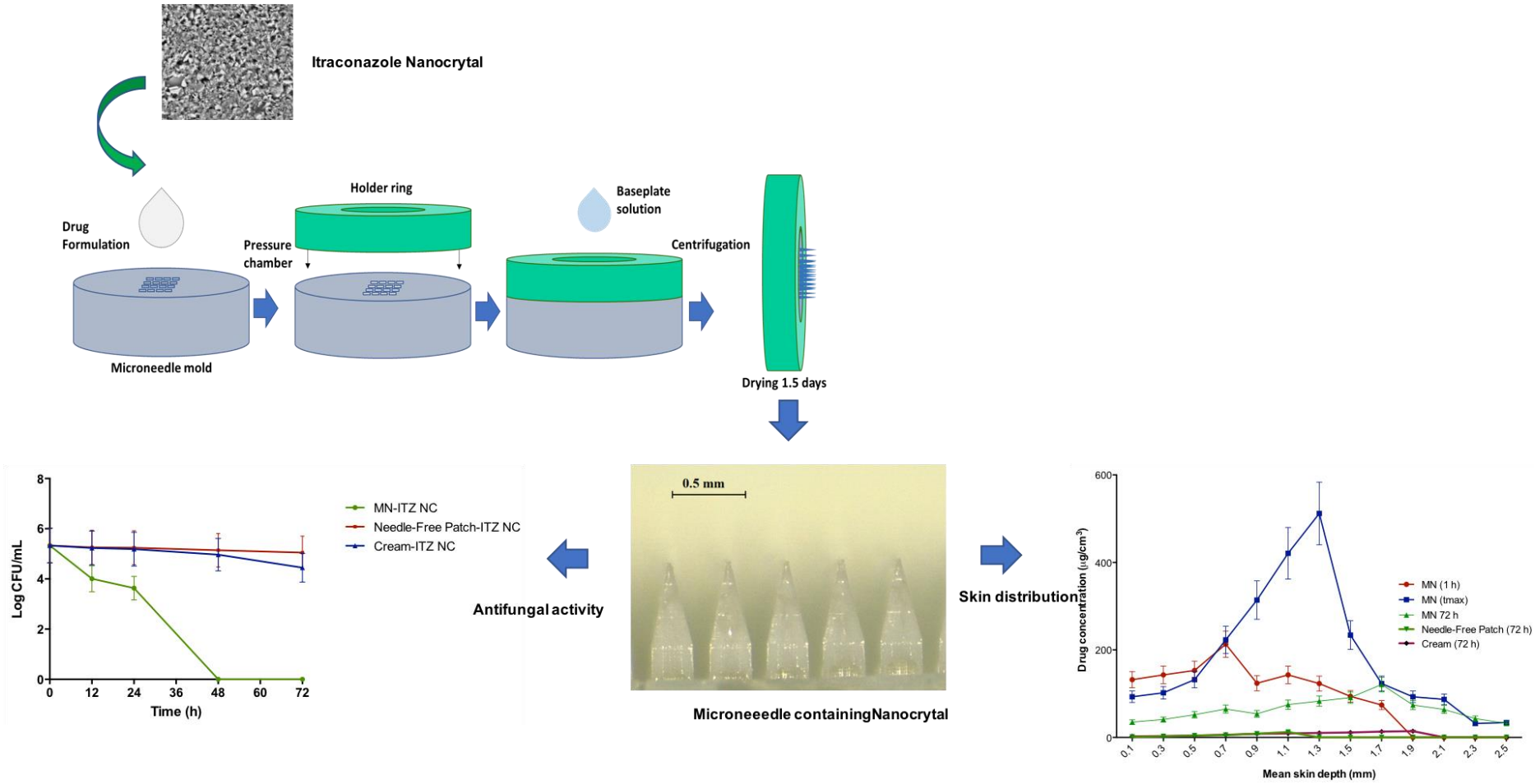

ABSTRACT

The administration of conventional dosage forms of itraconazole (ITZ) for cutaneous candidiasis treatment is limited by its poor aqueous solubility and the deep location of *Candida albicans* (CA) in this disease. In the present work, we developed a nanocrystal (NC) form of ITZ, which was incorporated into dissolving microneedles (MNs) to facilitate skin delivery of ITZ into the infection site. The NCs were prepared by media milling with an ultra-small-scale device using Pluronic®F127 as a stabiliser. The antifungal activity of ITZ was enhanced by NC formulations (MIC value of 2.5 μg/ml), compared to a coarse dispersion of ITZ (MIC value of > 2560 μg/ml). The formulation of ITZ into NCs increased dissolution rate by 3-fold. Furthermore, the dissolving MNs containing ITZ-NCs exhibited better dermatokinetic profiles, compared to needle-free patches and conventional creams containing ITZ-NCs. Importantly, the antifungal activity in an *ex vivo* candidiasis infection model exhibited that the CA viability declined by up to 100% after 48 h of administration. These studies have verified the concept that the incorporation of ITZ-NCs into dissolving MNs can offer an effective approach for cutaneous candidiasis treatment.

KEYWORDS

Itraconazole; nanocrystal; cutaneous candidiasis; microneedles; *Candida albicans*.

1. Introduction

The skin is the principal protective barrier of the human body. However, it is suspectible to various diseases, with fungal infections being a significant health problem globally [1]. It is estimated that around 1 billion infections occur every year, with *Candida spp.* being the most prevalent group of pathogens [2]. In particular, *Candida albicans* (CA) is responsible for approximately 70% of all *Candida spp* associated skin infections [3]. Furthermore, CA is reported to be able to invade the *stratum corneum*, resulting in systemic and occasionally, fatal infection [4]. In invasive fungal infections, CA is able to penetrate into the deeper layers of the skin, causing cutaneous human candidiasis, which is defined by dicrete ulcers that are mainly comprised of polymorphonuclear leukocytes [5].

The treatment for severe cutaneous candidiasis continues to be a significant challenge and is limited to a few types of drugs, mainly azoles derivates. However, their use in clinical applications is normally restricted because of toxicity issues [6,7]. Itraconazole (ITZ) is one of the triazole antifungals generally applied against a wide spectrum of fungal infections, including those induced by CA [8,9]. In comparison with other common antifungal drugs, ITZ has fewer nephrotoxic effects [10,11]. Importantly, ITZ exhibits better antifungal action and less drug resistance than other azole antifungal drugs, including ketoconazole, voriconazole and fluconazole [11]. Clinically, ITZ is given orally at doses between 200 mg and 400 mg daily to treat cutaneous candidiasis [8,12,13]. Importantly, oral administration of ITZ, yielding systemic exposure, has been associated with significant side effects, including cholestatic and hepatocellular damage [8,11]. In an attempt to reduce hepatotoxicity, ITZ could be delivered to the main infection site of cutaneous candidiasis which is the skin tissue [14]. However, the formulation of ITZ into topical dosage forms is limited by its high lipophilicity and extremely poor aqueous solubility (1 ng/ mL), therefore, causing the rare availability of ITZ topical dosage forms in the market [15]. Accordingly, a new approach to effective delivery of ITZ to the skin tissue is urgently required.

The formulation of nanocrystals (NCs) has become the strategy of preference for poorly soluble drugs with more than 20 products already approved in the market [16]. By definition, NCs are nanoparticles composed of up to 90% drug without any matrix material, and are usually surrounded by a stabiliser layer [17]. The key features of nanocrystals are an increased saturation solubility and dissolution rate, both related to their enlarged specific surface [18]. All these facts, together with a relative ease of production and scalability, make NCs a

promising strategy to incorporate hydrophobic drugs into various dosage forms [19]. Several drugs have been successfully developed into NCs-based approaches, including miconazole nitrate [20], azelaic acid [21], clarithromycin [22] and beclomethasone [23], showing that the formulation of such drugs into NCs could potentially increase their solubilities, providing a new strategy for hydrophobic drugs. However, even though the antimicrobial efficacy of nanoparticle delivery systems has been widely explored, the delivery of this system directly to the *cutaneous candidiasis* infection site in the skin has not been broadly studied. Therefore, a new delivery approach for antifungal drugs which can deliver the drug directly to the infection site is an interesting target to be explored.

Dissolving microneedles (MNs) are minimally invasive devices, by-passing the major skin barrier and, therefore, resulting in high localisation of drugs in the skin [24]. When this device is applied to the surface of the skin, it creates aqueous conduits with a number of small pores through which the drugs or the drug nanoparticles can reach the deeper layers of the skin [24,25]. Importantly, the use of MNs possesses several benefits, including painless delivery, the ability to achieve rapid delivery of drugs and compliant administration for the patient [26]. In addition, self-dissolvable nature of polymers used in the MN preparations provide other benefits, including the fact that such MNs do not generate biohazardous waste [27]. Specifically, several NC formulations have been incorporated into dissolving MNs to deliver drugs to the different layers of the skin, including curcumin [28], albendazole sulfoxide [24], rilpivirine [29] and cholecalciferol [30]. Therefore, taking into consideration the benefits of this delivery approach, the combination of NCs and dissolving MNs containing ITZ could be a beneficial option for treatment of cutaneous candidiasis, as this combination could potentially enhance both solubility and penetrability of ITZ.

In the present work, we specifically report for the first time the combination delivery system of ITZ-NCs and dissolving MNs for potential enhanced treatment of cutaneous candidiasis. The NCs were formulated and optimised using media milling using the ultra-small-scale device. The particle size, polydispersity index, shape and antifungal activity were also performed. Afterwards, the NCs were incorporated into dissolving MNs. Furthermore, *ex vivo* dermatokinetic studies were carried out in normal porcine skin to investigate the ability of this system to deliver ITZ intradermally. Lastly, the penetrability and the antifungal activity of the novel formulation were evaluated in *ex vivo* candidiasis infection models. The main

outcomes of these proof of concept works could potentially provide a new insight to solve the problem in the cutaneous candidiasis treatment.

2. Materials and Methods

2.1. Materials

Itraconazole (purity, ≥98%) of analytical grade was purchased from Tokyo Chemical Industry (Tokyo, Japan). Poly(vinyl alcohol) (PVA) (31–50 kDa), PVA (9–10 kDa) and Tween®80 were purchased from Sigma-Aldrich (Dorset, UK). Pluronic® F127 (P127) was obtained from BASF SE (Ludwigshafen, Germany). Poly(vinylpyrrolidone) PVP (58 kDa) was provided by Ashland (Kidderminster, UK). Ultrapure water was obtained from a water purification system (Elga PURELAB DV 25, Veolia Water Systems, Dublin, Ireland). Yttria stabilized zirconia beads of 0.5 mm diameter were purchased from Chemco Advance Material (Suzhou, China). All other reagents were of analytical grade and purchased from standard commercial suppliers.

2.2. Fabrication of ITZ-NCs

ITZ-NCs were prepared by media milling using the ultra-small-scale device described previously [31], with modifications. Briefly, 0.2 g of ITZ and 10 ml of 0.5, 1 and 2% v/w of Tween 80®, P127 or PVA were placed in a 12 ml glass vial. To create movement in the system, two magnetic bars of (12 x 6 mm) and 8 g of zirconia beads were added. Then, the system was closed with a hermetic lid, fixed to an IKA RCT Basic Magnetic Stirrer (IKA, Staufen, Germany), and agitated at 1000 rpm for 24 h. During this period (1 h, 2 h, 3 h, 4 h, 6 h, 8 h, 10 h, 12 h and 24 h), samples were withdrawn for particle size determinations. Afterwards, the obtained slurry was filtered through a mesh 200 sieve to separate the magnetic bars and zirconia beads from the nanosuspensions. Prior to dissolving MN preparations, the NCs were washed using distilled water by three cycles centrifugation at 14,000 rpm (Sigma® 1–14 micro-centrifuge, SciQuip Ltd., Shropshire, UK) for 30 min, forming washed NCs pellets.

2.3. Characterisation of ITZ-NCs

Particle size distribution and polydispersity index were determined by dynamic light scattering (DLS) using a NanoBrook Omni® analyser (Brookhaven, New York, USA). To this purpose, 5 µl of nanosuspension was manually dispersed in 4 ml of water and placed into plastic disposable cells. The equilibration time was set at 3 min and determinations were made at 25°C.

Results were expressed as mean values ± standard deviation (mean ± SD, n=3). In scanning electron microscopy (SEM) experiments, coarse ITZ or a droplet of ITZ nanosuspension (heated at 37 °C to dryness) were deposited onto adhesive carbon tape, and observed in a TM3030 microscope (Hitachi, Krefeld, Germany). Additionally, a Fourier transform infrared (FTIR) spectrometer (Accutrac FT/IR-4100™ Series, Perkin Elmer, USA) was utilised to investigate the possibility of ITZ to chemically interact with the compounds used in the formulation. Differential scanning calorimetry (DSC) measurement and X-ray powder diffraction of ITZ, ITZ-NCs and physical mixture (PM) of the optimised formulation were conducted using a differential scanning calorimeter (DSC 2920, TA Instruments, Surrey, UK) and an X-ray diffractometer (Rigaku Corporation, Kent, England), respectively.

2.4. In vitro release studies

The *in vitro* release studies of ITZ and ITZ-NCs were performed using a dialysis method [32]. ITZ (10 mg) and an amount of ITZ-NCs corresponding to 10 mg of ITZ were dispersed into the Spectra-Por®, 12,000–14,000 MWCO dialysis membrane (Spectrum Medical Industries, Los Angeles, CA, USA). The dissolution was performed at 37˚C and 100 rpm in 100 mL of PBS (pH 7.4) and 1% w/v of Tween 80. Aliquots of 1 mL were taken at predetermined time intervals and replaced with an equal volume of fresh release medium. To determine the amount of ITZ released from NCs, the samples were then analysed using HPLC after appropriate dilutions.

2.5. Drug release kinetic using mathematical modelling

Common mathematic models were applied to the percentage of drug released, as follows [27]:

Zero order: $Q_t = Q_0 + K_0 t$ Equation (5)

First order: $lnQ_t = lnQ_0 + K_1 \mathrm{t}$ Equation (6)

Higuchi: $Q_t = K_H\sqrt{t}$ Equation (7)

Korsmeyer-Peppas: $Q_t = K_t n$ Equation (8)

Hixson-Crowell: $Q_0^{1/3} - Q_t^{\frac{1}{3}} = K_s t$ Equation (9)

Where Q_t (%) is the percentage of drug released at time t, Q_0 is the initial value of Q_t, t is the time, n is the diffusion release exponent, K_0, K_1, K_H, K_t and K_s are the release coefficients corresponding to relevant kinetic models. DDSolver was utilised to calculate the model parameters.

2.6. In vitro antifungal activities

2.6.1. Culture of Candida albicans (CA)

CA NCYC 610 (stock of Microbiology Laboratory, School of Pharmacy, Queen's University Belfast, UK) was maintained at 4˚C. The fungi were cultivated in Saboaraud Dextrose Broth (SDB), at 37˚C and 100 rpm for 24 before antifungal activity studies. The collection of the fungal pellets was carried out by centrifugation at 3000 rpm for 30 minutes. The attained pellet was re-dispersed in fresh SDB. Following this, optical density of the fungal dispersions was set in order to obtain an equivalent to 1.5×10^7 CFU/mL at 550 nm.

2.6.2. Determination of minimum inhibitory concentration and minimum fungicidal concentration

A microtiter broth dilution method in 96-well bottom-plates was applied in determination of the minimal inhibitory concentrations (MIC) and minimal fungicidal concentrations (MFC) of ITZ in water (suspension form), ITZ in DMSO (solution form) and ITZ-NCs, according to the protocol of the Clinical and Laboratory Standards Institute [33]. In brief, 100 µL fungal suspension (1.5×10^7 CFU/mL) in SDB was mixed with 100 µL of various concentrations of ITZ in water, ITZ in DMSO and ITZ-NC, resulting in 7.5×10^6 CFU/mL of fungal. The microplates were incubated for 24 h at 37°C. Finally, the MIC was determined by observing the lowest concentration of ITZ in water, ITZ in DMSO and ITZ-NC at which no obvious growth of the fungus following incubation. For determination of MFC, 20 µL of dilutions from the MIC wells and the other wells with the concentration above the MIC were cultivated onto Saboaraud Dextrose Agar (SDA) plates and incubated for 24 hours at 37˚C. Subsequently, the fungal colonies on the plates were counted. The MFC was defined as the lowest concentration that eradicated 99.9% of the fungal growth [34].

2.6.3. Time kill assay

The determination of time-killing kinetics of ITZ and ITZ-NCs against CA was carried out as per the method described previously [35], with slight modifications. Briefly, concentrations equivalent to MIC, 2 x MICs and 4 x MICs of ITZ and ITZ-NC were prepared, and these dilutions were mixed with the fungal dispersions, forming 7.5×10^6 CFU/mL of CA. The fungal cultures were then cultivated at 37˚C for 24 h. Afterwards, 20 µL of the medium cultures were taken at 0, 2, 4, 6, 8, 12, 18 and 24 h and inoculated into SDA plates aseptically. Finally, the SDA plates were cultivated for 24 h at 37°C and the viable colony forming units (CFU) of CA were counted. The procedure was performed three times and a curve of the log CFU/mL against time-kill was created.

2.7. Fabrication of two-layered dissolving MNs

Two-layered dissolving MNs of ITZ-NCs were prepared using silicone moulds with needle density of 16 x 16, pyramidal needles; 850 µm height [600 µm pyramidal tip, 250 µm base column] and 300 µm width at base and 300 µm interspacing (Figure 1). The MNs matrix were prepared from an aqueous blend consisting of 15% w/w of PVA (31-50 kDa) and 25% w/w of PVP (58 kDa). In this study, five different formulations as the first layer of MNs were prepared, consisting of 10% *w*/*w* of washed pellets of ITZ-NC and 90% w/w of MN matrix polymer (formulation code 1 in each formulation); 20% *w*/*w* of washed pellets of ITZ-NC and 80% w/w of MN matrix polymer (formulation code 2 in each formulation); 30% *w*/*w* of washed pellets of ITZ-NC and 70% w/w of MN matrix polymer (formulation code 3 in each formulation); 40% *w*/*w* of washed pellets of ITZ-NC and 60% w/w of MN matrix polymer (formulation code 4 in each formulation); and 50% *w*/*w* of washed pellets of ITZ-NC and 50% w/w of MN matrix polymer (formulation code 5 in each formulation). In brief, the first layer was poured onto the moulds and placed in a positive pressure chamber and a pressure of 5 bar was applied for 2 mins. Afterwards, the excess of the formulation on the top of the moulds was removed with a spatula. A silicone ring with external diameter of 23 mm, internal diameter of 18 mm, thickness of 3 mm was connected to the MN moulds using an aqueous blend of PVA (9-10 kDa) 40% w/w as a glue. The formulations were then dried at room temperature for 6 h. Following this, 850 µL of the second layer, composed of mixture of an aqueous blend of PVP (90 kDa) 30 % w/w and glycerol 1.5 % w/w was poured inside the ring. Afterwards, the moulds were centrifuged for 15 min at 3500 rpm for 15 minutes. Finally, the MNs were dried at room temperature for 24 hours and at 37˚C for 12 hours. The MN morphologies were visually

observed using a Leica EZ4D light microscope (Leica Microscope, Milton Keynes, UK) and scanning electron microscope (SEM) TM3030 (Hitachi, Krefeld, Germany).

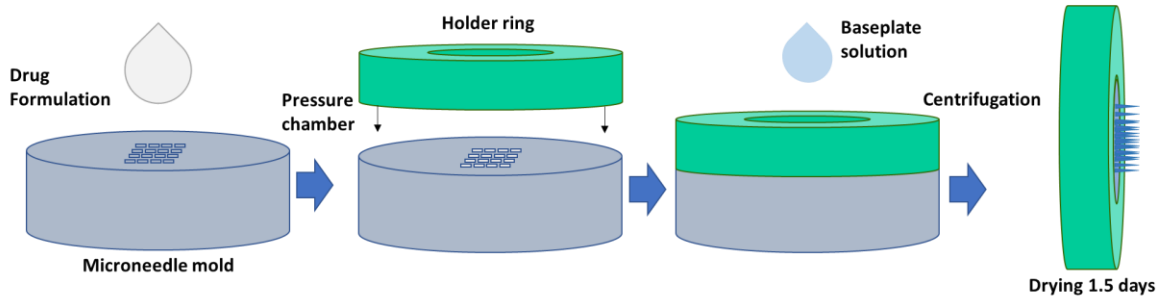

Figure 1. Schematic of dissolving MNs preparation

2.8. Evaluation of mechanical and insertion properties of dissolving MNs

A TA-TX2 Texture Analyser (Stable Microsystems, Haslmere, UK) was employed to evaluate the mechanical properties of dissolving MNs, as reported in a previous study [36]. Additionally, the ability of MNs to penetrate Parafilm®M as a validated skin-simulant artificial membrane was also studied using a method reported previously [37]. The penetration depth of MNs following insertion into Parafilm® M and full-thickness neonatal porcine skin (obtained from less than 24 post-mortem of stillborn piglet) was also determined using an optical coherence tomography (OCT) microscope (Michelson Diagnostics Ltd., Kent, UK), as reported previously [24,29,36]. To visualise needle insertion and depth of penetration, ImageJ® (National Institute of Health, Bethesda, MD, USA) software was utilised.

2.9. Calculation of drug content localised ~~to~~ in the needles

In an attempt to calculate the amount of ITZ in MN needles, the needles were separated carefully from the baseplate using a scalpel and dissolved in 5 mL chloroform. The mixture was sonicated in a bath sonicator for 1 h. The mixture was centrifuged for 15 min at 14,000 rpm. The quantity of ITZ in the supernatant was measured by HPLC.

2.10. Redispersion of ITZ-NCs from MN formulations

The MNs containing ITZ-NCs were dispersed in the distilled water. Following this, the characteristics of NC, namely particle size and PDI were determined using DLS. The results obtained were compared to the initial characteristics of NC.

2.11. Dissolution studies

In order to evaluate the dissolution time of MNs the *in situ* in the excised full-thickness neonatal porcine skin, the MN arrays were inserted into the skin section using manual pressure [26]. To ensure the MNs stayed in the same place, a cylindrical stainless-steel weight (5.0 g) was placed on the top of the MNs. MN were detached from the skin at a different interval times and the morphology of MNs was observed using the Leica EZ4 D stereo microscope.

2.12. Ex vivo dermatokinetic studies

Ex vivo dermatokinetic studies of MNs containing ITZ-NC were carried out in excised full-thickness porcine skin, as per a method reported in our previous studies [24,27]. Briefly, using cyanoacrylate glue, the skin was first joined to the donor section of the Franz cell diffusion cells. The MNs were inserted into the skin using manual force for 30 s, and the donor section was attached to the receiver chamber containing PBS (pH 7.4) and 1% w/v of Tween 80 to ensure the maintenance of sink conditions. Afterwards, the cylindrical stainless-steel weight (5 g) was located on top of the MNs. To avoid the evaporation of the medium, the sampling arm and the donor compartment were sealed using Parafilm®M. The temperature of the receiver chamber was kept at 37 ± 1°C. The chamber was stirred at 600 rpm. At various interval time points, the MNs were detached, and the skin was rinsed thrice with distilled water to remove any excess formulation. Afterwards, a biopsy punch (5 mm diameter) (Stiefel, Middlesex, UK) was utilised to obtain skin sections. The skin sections were heated for 2–3 min in a water bath at 60 °C. The epidermis sections were further detached from the dermis sections using tweezers. To extract ITZ from the skin samples, 1 mL chloroform was added into samples and homogenised at 50 Hz using Tissue Lyser LT for 10 min (Qiagen, Ltd., Manchester, UK). The amount of ITZ in the supernatant was determined using HPLC. To analyse the dermatokinetic profiles, PKSolver (China Pharmaceutical University, Nanjing, China) [38] was utilised with one-compartment open model after the construction of a curve consisting of drug concentration versus time. Several dermatokinetic parameters were observed, namely the maximum drug concentration (C_{max}), the time of maximum concentration (t_{max}), the drug concentration time curve from time zero (t = 0) to the last experimental time point (t = 72 h) (AUC), the mean half-life ($t_{1/2}$) and the mean residence time (MRT). As a comparison, needle-free patches and conventional cream containing ITZ-NC were made and the dermatokinetic studies were also performed for them.

In order to evaluate drug distribution and deposition in the different layers of skin, samples were taken after 1 h, dermis t_{max} from the dermatokinetic study and 72 h. Afterwards, the skin samples were quick-frozen in liquid nitrogen. The frozen samples were sectioned into 50 μm thickness using a Leica CM1900 Cryostat (Leica Microsystems, Nussloch, Germany) and four consecutive sections were put into a microtube. This step was repeated until the entire skin was sectioned. Then, 500 μL of chloroform was added to the skin sections. To dissolve the drug, the sample was vortexed for 30 min. Finally, the sample was centrifuged at 14,000× *g*, 15 min and the supernatant were collected and analysed using HPLC method.

2.13. Antifungal activity in an ex vivo fungal infection model in porcine skin

2.13.1. Preparation of fungal infection model on porcine skin

The skins were disinfected by immersing in 70% ethanol for 1 hour. The skin was allowed to dry in a biosafety cabinet for 20 min prior to the experiment [39]. Briefly, 50 μL of the fungal suspensions of 1.5×10^7 CFU/mL was injected intradermally into the sterilised skin. The skin pieces were aseptically placed on SDA plates. The plates were cultivated at 37°C with the skin were aseptically moved to fresh SDA plates every day for 7 days.

2.13.2. Antifungal activity in ex vivo fungal infection model on porcine skin

Antifungal activity in the *ex vivo* fungal infection model in porcine skin was carried out using similar apparatus to the dermatokinetic studies. In this study, instead of the using normal full-thickness porcine skin, the skin infection model was placed in the Franz diffusion cells. After 12 h, 24 h, 48 h and 72 h of the application of MNs, the skin samples were collected, and 1.5 mL sterile water were added to the skin in microtubes. The mixture was then homogenised at 50 Hz using a Tissue Lyser LT (Qiagen, Ltd, Manchester, UK) for 15 min. Afterwards, 20 μL homogenised samples were inoculated into SDA plates and were incubated for 24 h at 37°C. Additionally, as a comparison, needle-free patches and conventional cream containing ITZ-NC were also applied to the infected skin and the same technique was carried out. The numbers of viable CFU were finally counted. Infected skin without any treatments was utilised as a positive control.

2.14. Instrumentation and chromatographic condition for analytical method

The concentrations of ITZ in each study were determined by HPLC (Agilent Technologies 1220 Infinity UK Ltd, Stockport, UK). The analyses were performed using a Phenomenex® Luna C_{18} (ODS1) column (150 mm × 4.6 mm i.d. with 5 µm particle size) with the flow rate of 1 mL/min. A mixture of acetonitrile and 25 mM ammonium acetate buffer (65:35 *v*/*v*) pH 5 was used as the mobile phase and the analyses were performed using a UV detector at 270 nm. The volume of injection was 50 µL and the analyses were performed at ambient temperature. This method was validated following the guidelines of the International Committee on Harmonisation (ICH) 2005.

2.15. Statistical analysis

All results were reported as means ±standard deviation (SD). GraphPad Prism® version 6 (GraphPad Software, San Diego, California, USA) was utilised to statistically analyse the results. To compare two cohorts, an unpaired t-test was utilised. To compare several cohorts, the Kruskal-Wallis test with post-hoc Dunn's test was utilised. p value < 0.05 denoted a significant difference.

3. Results and Discussion

3.1. Fabrication and characterisations of ITZ-NCs

Before the incorporation of ITZ in the MN formulations, it was transformed into NCs by media milling using an ultra-small-scale approach. As observed in Figure 2.1, Tween® 80 when used at concentrations of 0.5, 1 and 2% generated particle sizes in the nanometer range only after 10 h. Furthermore, after 24 h the particle sizes were 782 ± 86 nm, 598 ± 65nm and 573 ± 69 nm for 0.5, 1 and 2%, respectively. Nevertheless, the obtained PDI values were > 0.3 in all cases, indicating the presence of multiple particle size populations, which could lead to Ostwald ripening and thus to physical instability [40]. It is important to note that the instability of nanoformulations caused by Ostwald ripening only occurs in the liquid state. In order to achieve stable nanoformulations, the complete drying of the nanoparticles is necessary [41]. Therefore, the incorporation of NCs into a dry and solid dosage form, dissolving MNs, could be beneficial to obtain stable NC formulations. Similarly, when PVA was used as stabiliser, the media milling experiment produced NCs with a similar comminution trend and final PDI values greater than 0.4 as observed in Figure 2.2. In this case, the final particle sizes at different

PVA concentrations were 0.5%, 983 ± 108 nm; 1%, 632 ± 69 nm and 2% 463 ± 56 nm. When nanosuspensions were prepared with P127 (Figure 2.3), the nanometer range was achieved at 6 h and the final particle sizes after 24 h were 499 ± 55 nm, 320 ± 35 nm and 324 ± 36 nm for P127 concentrations of 0.5, 1 and 2% respectively. However, the milling time of 8 h with 1% P127 resulted particle sizes of 352 ± 38 nm with PDI of 0.37 ± 0.03. Analysed statistically, the results obtained after 8 h milling time with 1% P127 were not significantly different ($p > 0.05$) when compared to 2% P127 and to further milling time. Furthermore, P127 allowed obtaining the lowest PDI values, which corresponded with monodisperse and narrowly distributed particle sizes. Poloxamers have been previously described as effective stabilisers in nanosuspensions of highly hydrophobic drugs. This is related to their ability to efficiently orientate their hydrophobic moieties to the NC surfaces, while exposing their hydrophilic regions to the aqueous solvent [42]. With these results in consideration, and aiming at minimizing the processing time and amount of stabiliser, the formulation corresponding to P127 1% w/v and a milling time of 6 h was selected for the further studies.

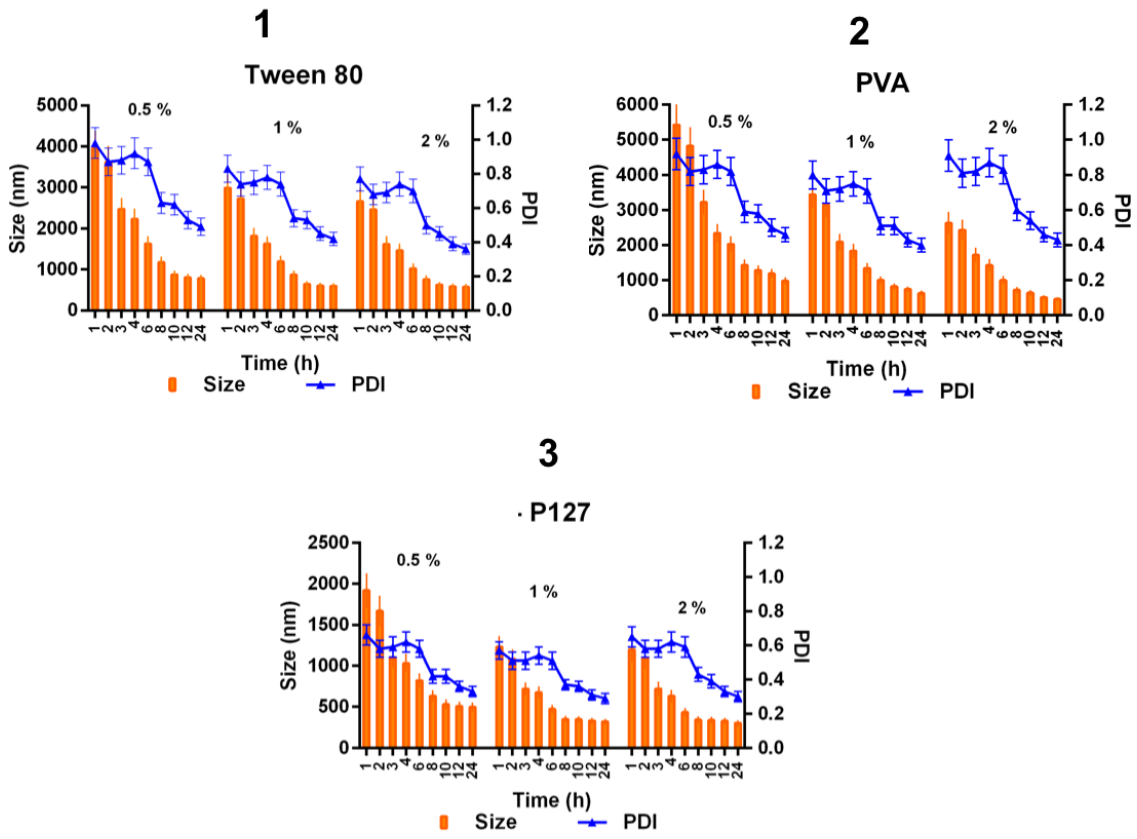

Figure 2. Particle size and PDI determinations of the ITZ nanosuspensions prepared with Tween 80 (**1**), PVA (**2**) and P127 (**3**) at 0.5, 1 and 2 % w/v (means ± SD, $n = 3$).

Figure 3.1 and 3.2 show the SEM images of pure ITZ and ITZ-NCs, respectively. The NC sizes found in this experiment were similar than those observed in DLS analysis (~300 nm). Figure 3.3 shows the FTIR spectra of ITZ, PM and ITZ-NCs. The spectra clearly confirmed that there were no interactions between ITZ and excipient used to prepare the NCs. The strong signal observed at 1697 cm^{-1} can be attributed to imine group C=N stretch (1690 – 1650 cm^{-1}) and to N-C=O stretch (1680 – 1630 cm^{-1}). The next stretch found at 1509 cm^{-1} can be attributed to C=C, characteristic from aromatic ring (1600 – 1475 cm^{-1}). The peak at 1217 cm^{-1} was due to C-N stretching (1350 – 1000 cm^{-1}). Additionally, the stretch observed at 1184 cm^{-1} can be attributed to C-O functional group (1300 – 1000 cm^{-1}) and 823 cm^{-1} stretching refer to *para* aromatic ring-substituted (870 – 800 cm^{-1}) present in ITZ. Finally, the 671 cm^{-1} stretching refer to C-Cl present in *ortho* and *para*-substituted in the aromatic ring (785 – 540 cm^{-1}). All the characteristic peaks in ITZ spectra were also found in the PM and NCs formulation, indicating no interaction between the drug and P127.

DSC thermal analysis was performed to evaluate the physicochemical interaction between any compounds and to determine whether the crystallinity was kept after the milling technique process. The thermograms from ITZ, PM and ITZ-NCs are shown in Figure 3.4. All endothermic peaks remained sharp at 163°C, representing the ITZ melting point and crystallinity in ITZ, ITZ-PM, and ITZ-NCs, indicating that the nanotechnology process applied, and excipients used did not interfere in the physicochemical properties of ITZ. The crystallinity was also confirmed by XRD analysis, showing sharp characteristics peaks at 2θ values of 14.85, 18.01, 20.32 and 23.92 in ITZ, PM and ITZ-NCs, respectively (Figure 3.5).

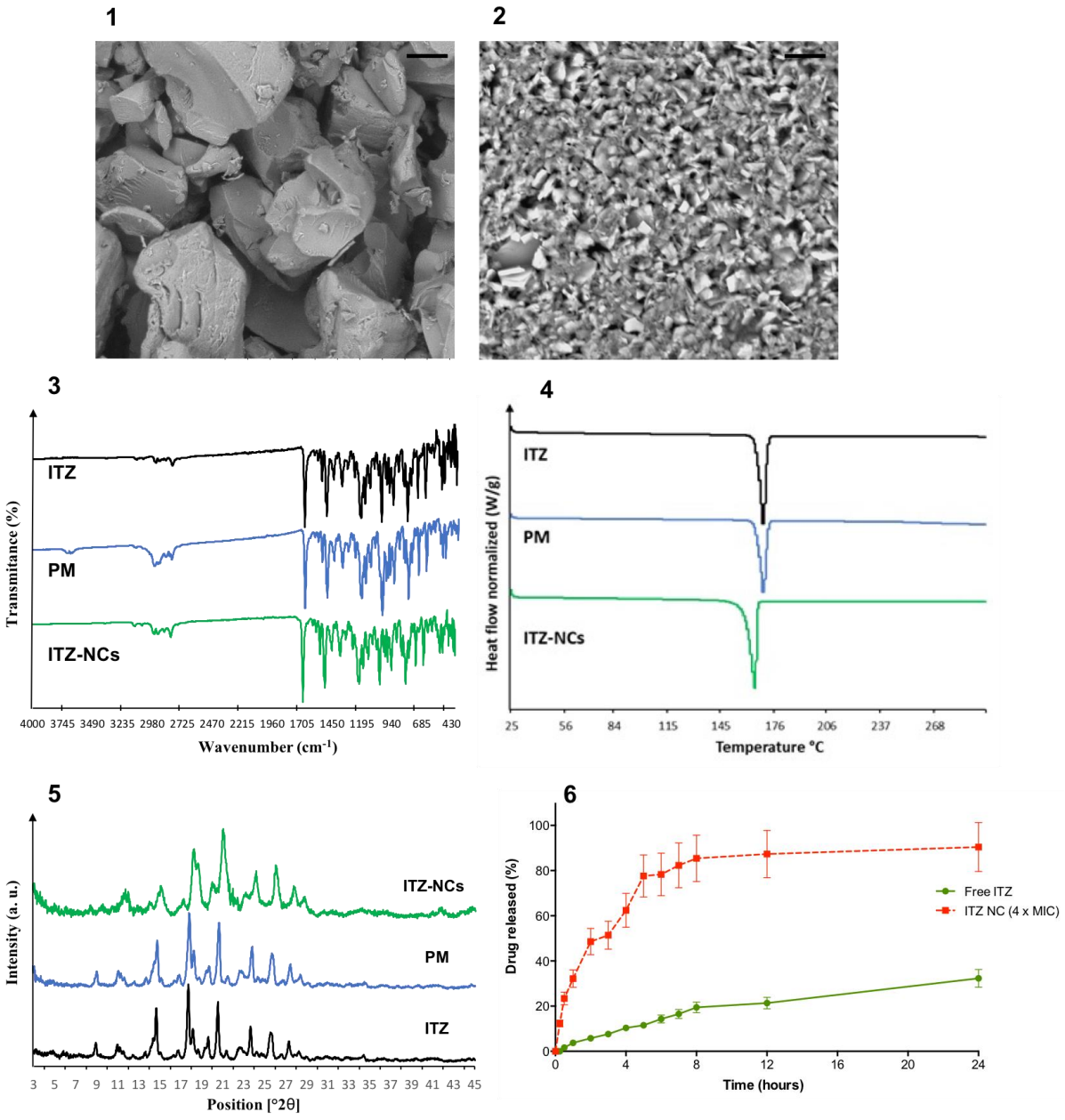

386

387 **Figure 3.** SEM images of pure ITZ (**1**) and ITZ-NC (**2**) at a magnification power of 30000x (The black scale bar
388 represents a length of 1 µm in each case). FTIR spectra of ITZ, PM and ITZ-NC (**3**). DSC thermogram of ITZ,
389 PM and ITZ-NC (**4**). X-ray diffractogram of ITZ, PM and ITZ-NC (**5**). *In vitro* release profiles of ITZ-NC in
390 comparison with the coarse ITZ (means ± SD, $n = 3$) (**6**).

391

392 *3.2. In vitro release study*

393 The *in vitro* release behaviour of ITZ in comparison with its NCs formulation is presented in
394 Figure 3.6. According to this study, the formulation of ITZ into NCs enhanced the release
395 behaviour of the drug. The experiment showed that 90.41± 17.32% of ITZ was released from
396 the nanocrystalline formulation after 24 h. Conversely, the amount of drug released from coarse

ITZ was approximately three times lower (31.96 ± 6.11%). Analysed statistically, the release rate at 24 h of ITZ-NCs was significantly higher (p = 0.011) than that of the free ITZ. This behaviour is related on one hand, with the enlarged specific surface of NCs, which leads to an increase in the dissolution rate [42,43] and, on the other hand, to a greater particle curvature, which is associated with an increment in the saturation concentration [18].

3.3. Drug release kinetic using mathematical modelling

To further understand the mechanism of release, common mathematic kinetic models were applied to the release profiles obtained. The most appropriate release model was chosen according to the correlation coefficient value. The correlation coefficient values were found to be 0.67, 0.98, 0.78, 0.81 and 0.66 for Zero-order, First-order, Higuchi, Korsmeyer-Peppas and Hixson-Crowell, respectively. As per the result, the release behaviour of ITZ-NCs formulation followed the First-order kinetic model best. Therefore, the release of ITZ from the formulation depends on the concentration of ITZ in the NC formulation [24,44].

3.4. In vitro antifungal activity

3.4.1. Determination of minimum inhibitory concentration and minimum fungicidal concentration

Three treatments, namely ITZ–water, ITZ–DMSO and ITZ-NCs were tested on CA. In this study, two forms of free ITZ were evaluated, namely dispersion form in water and solution form in DMSO. The comparison of MIC and MFC values between free ITZ and ITZ-NCs are shown in Table 1. The results showed that ITZ in the suspension form in water exhibited less antifungal activity, compared to ITZ-DMSO and ITZ-NCs. This might be caused by the insolubility of ITZ in water and, consequently, reduced ability to penetrate the CA cell membrane. It has been reported that the antifungal mechanism of ITZ is based on inhibition of lanosterol 14-α-methylase, the fungal CYP450 dependant enzyme, in the cell membrane of the fungus [45]. Accordingly, to effectively show its antifungal activity, ITZ must be able to exhibit an adequate penetration into the cell membrane which could not be achieved by ITZ dispersion in water [46]. On the other hand, ITZ in solution form showed profound antifungal activity against CA presumably due to the ability of ITZ to penetrate the CA cell membrane effectively. Notably, our control study using DMSO alone did not exhibit antifungal activity. Interestingly, the NCs-based formulation exhibited an antifungal activity comparable to that of the ITZ solution. This might be caused by the enhancement of the aqueous solubility of ITZ

following nanocrystallisation, improving the ability of ITZ to effectively penetrate the CA cell membrane [47]. Furthermore, MFC values were determined. In all cases, MFC values were greater than MIC, demonstrating that greater concentration of ITZ was needed to kill the fungal cultures. Importantly, the ratio of MFC to MIC was < 4. A ratio of ≤ 4 exhibits fungicidal activity and a ratio of > 4 exhibits fungistatic activity [48]. Our study suggested that to show fungicidal activity, ITZ should be in the form of solution or NCs formulation. However, due to the insolubility of ITZ, it is impossible to prepare dosage forms containing ITZ in the solution form. Therefore, our approach of preparing ITZ into a NCs-based formulation, could be beneficial, as it showed similar antifungal activity to ITZ solution.

Table 1. MIC and MFC values of free ITZ in water, free ITZ in DMSO and ITZ-NCs (n= 3)

	MIC (µg/mL)	**MFC (µg/mL)**
Free ITZ-water	> 2560	> 2560
Free ITZ-DMSO	2.5	5
ITZ-NCs	2.5	5

3.4.2. Time kill assay

Time kill assays were performed to further investigate the time needed by ITZ to completely kill CA. The curves of the time kill of free ITZ in DMSO and ITZ-NCs against CA are depicted in Figure 4. The CA viable colony forming units improved by around 6.9 log CFU after 24 h cultivation time in the untreated group. With MIC values, after 24 h, the solution of ITZ and ITZ-NCs could not kill 99.99% of CA culture. Essentially, when 2 times the MIC values were evaluated, there were no viable CA culture found after 18 h and 24 h in the case of ITZ solution and ITZ-NCs, respectively. More importantly, the time required to kill 100% of CA culture declined to 12 h and 18 h following incubation with 4 times the MIC values of ITZ solution and ITZ-NCs, respectively. The outcomes attained in this study suggested that the killing rates of ITZ in the NC-based formulations depended on the concentration of ITZ in the fungal culture media.

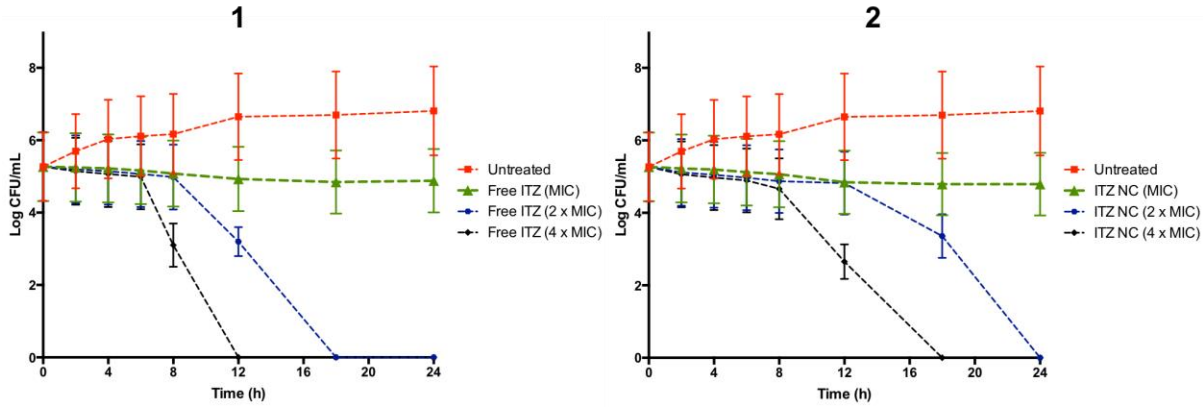

Figure 4. Time kill assay of free ITZ (1) and ITZ-NC (**2**) against *Candida albicans* (means ± SD, *n* = 3).

3.5. Fabrication of two-layered dissolving MNs

In this study, the MNs were formulated using an aqueous blend of PVP and PVA. Our previous study showed that the combination of these water soluble polymers in the MN formulations were able to form MNs with better mechanical properties in comparison with the use of single polymer, due to the formation of hydrogen bond amongst C = O groups of PVP and -OH groups of PVA [27]. Additionally, different concentrations of washed ITZ-NCs pellets were added in order to attain the highest possible drug loading for this approach. In this study, two-layered dissolving MNs were prepared by localising the ITZ-NCs in the MNs needles tips and pre-cast dry baseplates fabricated from 30% w/w PVP (360 kDa) and 1.5% w/w glycerol were utilised to support the needles. The formulation of two-layered MNs exhibits many advantages. In our preliminary studies, the fabrication of dissolving MNs containing ITZ-NCs in whole MNs did not show adequate mechanical characteristics, implied by fractured of the baseplate after the mechanical characterisation studies. Accordingly, to support the MNs needles, the utilisation of different base baseplates possessing adequate mechanical properties were required. Moreover, this type of formulation is able to avoid drug waste as a hydrophobic drug is unlikely permeating from baseplate part of MNs. Particularly, this method is favourable in industrial scale-up [27]. Figure 5.1 and 5.2 present the morphology of MNs containing ITZ-NCs obtained by a light microscope and a SEM. All formulations showed homogenous polymer mixtures with the MNs formed possessing sharp needle tips. Consequently, the mechanical and insertion properties of all MN formulations were then evaluated.

3.6. Evaluation of mechanical and insertion properties of dissolving MNs

Mechanical properties evaluation was conducted to investigate the ability of dissolving MNs to resist compression. Essentially, the ability of MNs to penetrate the skin is an important characteristic in MNs application. To assess the mechanical properties of the MN formulations, the heights of initial MN needles were compared to the needle heights following the application of 32 N/MN array [37]. Figure 5.3 shows the height reduction percentage of all MN formulations, representing the mechanical properties of MNs. The height reduction percentage were 11.21 ± 2.24% for F1, 11.19 ± 2.13% for F2, 11.32 ± 3.22% for F3, 12.43 ± 2.45% for F4 31.32 ± 6.54% for F5. Analysed statistically, the percentage of needle height reductions of F1, F2, F3 and F4 were not significantly ($p > 0.05$) different. However, the increase of ITZ-NC concentration to 50% w/w (Formulation E) caused a significant decrease ($p > 0.05$) in MN mechanical strength, indicated by the highest percentage of needle height reduction. Accordingly, the concentration of drug influenced the mechanical characteristics of dissolving MNs.

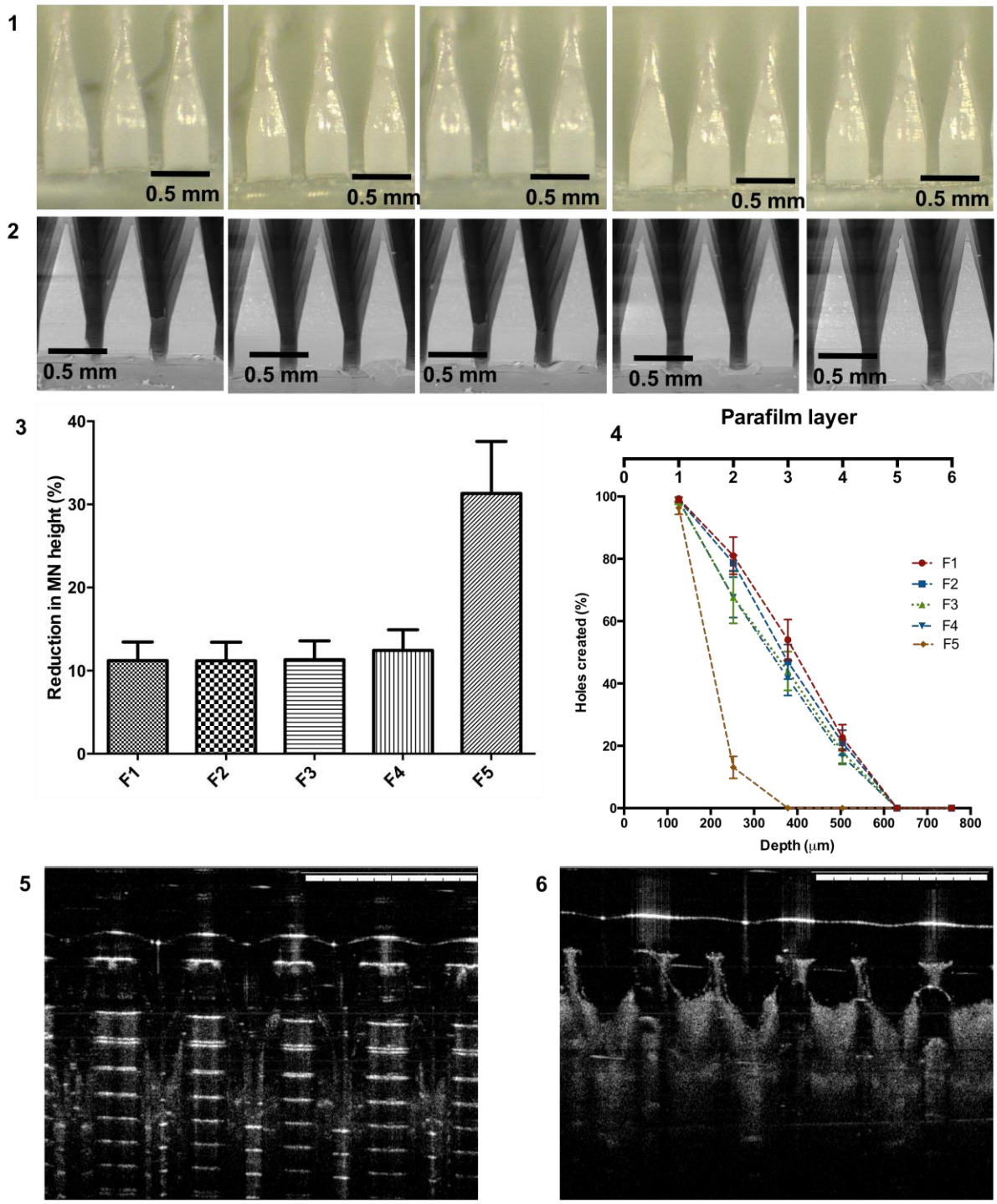

Figure 5. Light microscope images (**1**) of the MN formulations containing 10% ITZ-NC (F1) (**a**), 20% ITZ-NC (F2) (**b**), 30% ITZ-NC (F3) (**c**), 40% ITZ-NC (F4) (**d**) and 50% ITZ-NC (F5) (**e**). SEM images (**2**) of the MN formulations containing 10% ITZ-NC (F1) (**a**), 20% ITZ-NC (F2) (**b**), 30% ITZ-NC (F3) (**c**), 40% ITZ-NC (F4) (**d**) and 50% ITZ-NC (F5) (**e**). The percentage height reduction of needles on the MN arrays formulated containing different concentration of ITZ-NC (means ± SD, n = 3) (**3**). Percentage of holes created in Parafilm®M layers, using an insertion force of 32 N/array for MN formulations containing different concentration of ITZ-NC (means ± SD, n = 3) (**4**). Representative OCT images of F4 after insertion into Parafilm®M film (**5**) and full-thickness porcine skin (**6**). The scale bar represents a length of 1 mm in each case.

To further evaluate the ability of dissolving MNs to be inserted in the skin, Parafilm®M was employed as a validated skin stimulant. This prototypical has been developed by our research group to imitate human skin in MN insertion evaluation [37]. Figure 5.4 shows the result of MN insertion studies. The results obtained here were in a good agreement with the results of the mechanical properties evaluation. There was no statistical difference ($p > 0.05$) in insertion properties of F1, F2, F3 and F4. By observing the number of holes created in each layer of Parafilm®M, it was seen that all four formulations arrays could penetrate the Parafilm®M until four layers (504 µm), implying that approximately 54% of the MN needles lengths were inserted. On the other hand, F5 containing 50% w/w of washed NC pellets were only able to penetrate two layers of Parafilm®M, indicating poor insertion properties. Following on from these results, F4 with the highest drug loading (40% w/w) possessed adequate mechanical and insertion ability in Parafilm®M were chosen for further evaluation. In this study, the insertion visualisation in the Parafilm®M and the full-thickness neonatal porcine skin were both evaluated. The OCT image of the insertion profile of F4 into the Parafilm®M and the full-thickness neonatal porcine skin are exhibited in Figure 5.5 and 5.6. The results depicted that the depth of penetration of F4 was observed to be 503.91 ± 21.43 µm into Parafilm®M and 501.22 ± 14.42 µm into the full-thickness porcine skin. These values were in good agreement with the results found in the insertion evaluation by observing the percentages of holes created in Parafilm®M. OCT is a valuable technique in confirming MN insertion and studying depth of insertion as shown previously in different works [30,36,49–52].

3.7. Calculation of drug content localized to the needles

Following drying, the amount of ITZ localised in MN needles was quantified. The results showed that 3.29 ± 0.45 mg of ITZ were localised in F4 formulations. Therefore, this amount determind the dose of ITZ in one dissolving MN in the following evaluations.

3.8. Redispersion of ITZ-NCs from MN formulations

In the combination approach of nanotechnology and MNs, the particle properties, particularly particle size and PDI, should not be affected by MN formulations. In our study, following MN manufactures, the particle size and PDI of ITZ-NC in F4 were found to be 367 ± 33 nm and 0.32 ± 0.02, respectively. These properties were not statistically different ($p > 0.05$) compared to the initial properties of ITZ-NC.

3.9. Dissolution study

The F4 needles were completely dissolved after 30 min, with needles partially liquefied and a decrease in height were visualised after 10 min (Figure 6).

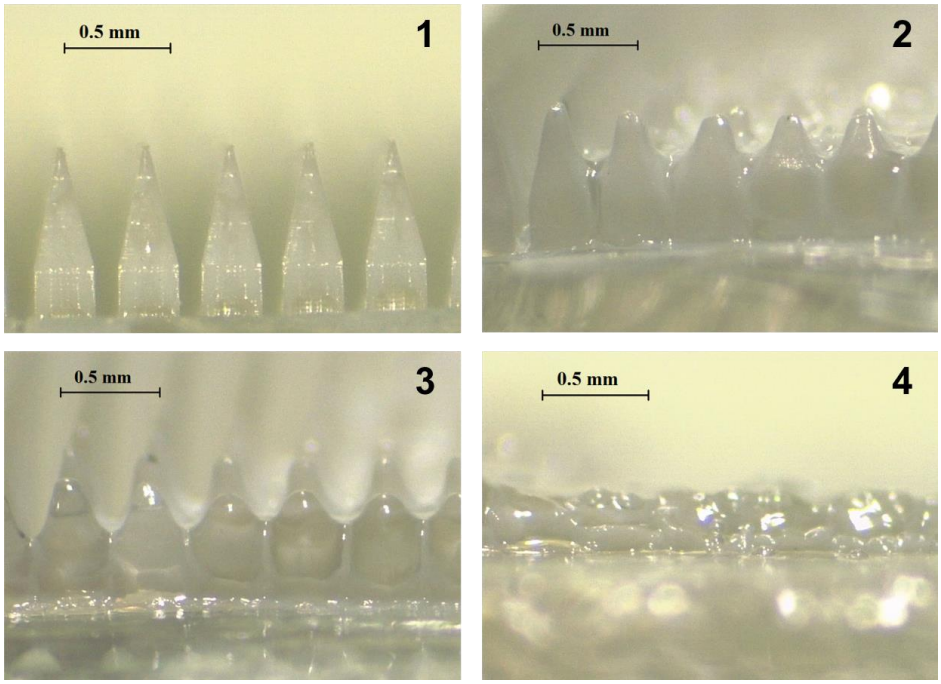

Figure 6. Digital micrographs of the dissolution of F4 at 0 min (**1**), 10 min (**2**), 20 min (**3**) and 30 min (**4**), following insertion into and removal from excised neonatal porcine skin *in vitro.*

3.10. Ex vivo dermatokinetic studies

The principal purpose of this study was to deliver the ITC-NC into the deeper layers of the skin, where CA colonises, infects the skin and causes cutaneous candidiasis [4]. Accordingly, it was critical to investigate the kinetic profile of ITZ after the administration of dissolving MNs containing ITZ-NC to the skin. In an attempt to accomplish this, a dermatokinetic analysis was designed and performed. This method has been successfully applied in our previous works to investigate the skin kinetic profiles of several drugs [24,27,39]. In the present work, the dermatokinetic profile of our combination approach was compared to needle-free patch and conventional cream as normal approaches to treat cutaneous candidiasis. The results showed that the concentration of ITZ in both the epidermis and dermis layers following the administration of dissolving MNs was statistically higher ($p < 0.05$) than the concentration of ITZ following the administration of needle-free patches and conventional creams, indicating the successful skin delivery using this combination approach compared to conventional dosage forms. The concentrations of ITZ in epidermis and dermis layers of the skin after the

application of dissolving MNs in comparison with needle-free patches and conventional creams are illustrated in Figure 7.1 and 7.2. The mean peak ITZ concentration (C_{max}) in the epidermis and dermis after the application of dissolving MNs were 543.46 ± 187.12 µg/cm^3 and 1973.12 ± 323.34 µg/cm^3, respectively. The times required to achieve C_{max} (t_{max}) were found to be 2 h and 3 h in the epidermis and the dermis after MN application, respectively. The area under curve (AUC_{0-24}) of ITZ were observed to be 10797.37 ± 2753.43 h.µg/cm^3 in the epidermis and 70411.12 ± 21321.32 h.µg/cm^3 in the dermis, respectively. The values of C_{max} and AUC_{0-24} in the epidermis were statistically lower ($p < 0.05$ each) than in the dermis. Essentially, in all parameters, the values of all dermatokinetic profiles of ITZ in the epidermis and dermis following the application of dissolving MNs were statistically greater ($p < 0.05$) than those following the application of needle-free patches and conventional creams. The dermatokinetic profiles of ITZ after conventional cream application were significantly higher ($p < 0.05$) compared to needle-free patches. The results presented in the present work revealed that the combination approach of NC and dissolving MNs could potentially enhanced the delivery of ITZ into the skin, resulting in the high retention of ITZ in the skin, where CA colonises, indicated by higher AUC values compared to other dosage forms.

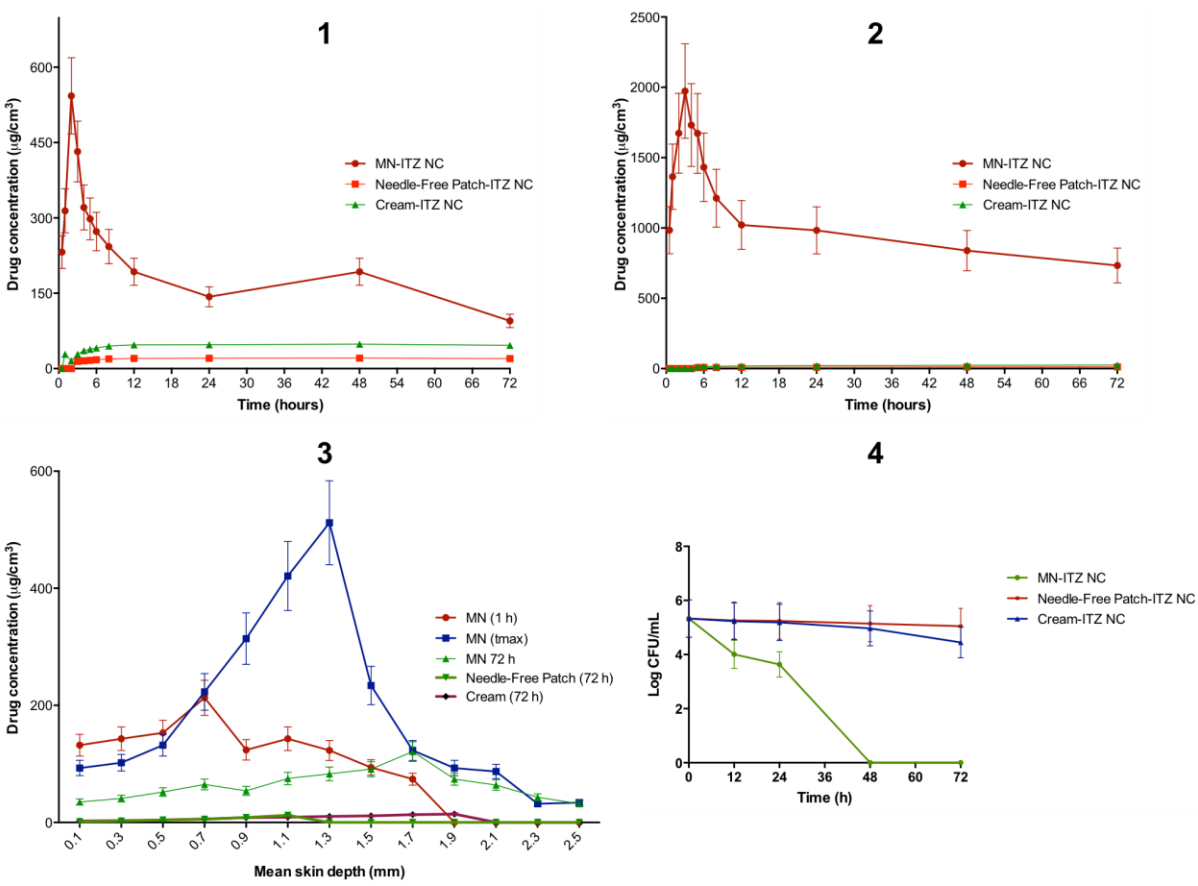

Figure 7. The concentration and time profile of ITZ in epidermis (**1**) and dermis (**2**) layers of excised full-thickness neonatal porcine skin, after the administration of dissolving MNs, free-needle patches and conventional cream containing ITZ-NC (means ± S.D., *n* = 3). The concentrations of ITZ in a different layer of neonatal porcine skin, after the administration of dissolving MNs, free-needle patches and conventional cream containing ITZ-NC (means ± S.D., *n* = 3) (**3**). *Candida albicans* viability (log CFU/mL) on in *ex* candidiasis infection models model in porcine skin after the administration of dissolving MNs, free-needle patches and conventional cream containing ITZ-NC (means ± S.D., *n* = 3). At 12, 24 h, 48 h and 72 h after-application, *ex vivo* infected skin were homogenised in sterile water and cultured onto SDA at 37 °C overnight (**4**).

The distribution profiles of ITZ in full-thickness porcine skin were further evaluated. The amount of ITZ distributed per cm^3 in different depths of skin and following various administration times, namely 1 h, t_{max} of dermatokinetic profiles and 72 h, are depicted in Figure 7.3. The results revealed that ITZ was distributed in the skin down to a depth of 2.5 mm in the case of dissolving MNs, 1.1 mm in the case of the needle-free patch and 1.9 mm in the case of the conventional cream. Essentially, the ITZ was detected in the skin deeper layers than the penetration depth of MN needles (around 500 µm), showing the movement of ITZ-NC in the skin. Specifically, following the application of dissolving MNs, ITZ reached a peak at a depth of 0.7 mm, 1.3 mm and 1.7 mm after 1 h, t_{max} and 72 h, with a concentration of 213.97 ± 46.61 µg/cm^3, 512.65 ± 103.43 µg/cm^3 and 121.03 ± 21.33 µg/cm^3, respectively. In contrast, statistically lower ($p > 0.05$) concentration of ITZ after the application of needle-free patches

and conventional creams were observed, indicating the poor skin distribution following their applications, compared to the skin distribution profiles of ITZ after the application of MNs. The higher distribution of ITZ after intradermal application of the dissolving MNs containing NC, compared to other conventional dosage forms, could improve the activity of ITZ to kill CA which are distributed in the different skin layer in cutaneous candidiasis diseases.

3.11. Antifungal activity in ex vivo fungal infection model on porcine skin

Lastly, with the aim to verify the effectiveness of this combination delivery system, we assessed the fungal burden in an *ex vivo* candidiasis infection models by viable cell counts. As shown in Figure 7.4, the fungal burden in *ex vivo* skin infection model increased by approximately 7.3 log CFU without any treatments. After 48 h from the application of needle-free patches, the fungal bioburden did not decrease significantly ($p > 0.05$) and this application was only able to kill 48% of fungal burden after 72 h. In the case of conventional cream application, due to the better dermatokinetic profile compared to needle free patches, this application could significantly decrease ($p < 0.05$) the fungal burden after 48 h and resulted in around 82% killing of the fungal burden. On the other hand, remarkably, following the application of dissolving MNs containing ITZ-NCs, the fungal burden decreased significantly ($p < 0.05$) after only 12 h and 100% of the fungal burden were killed after 48 h. Accordingly, these results revealed that the incorporation of NCs into dissolving MN formulations enhanced not only dermatokinetic parameters of ITZ, but also statistically improve the killing time and the fungal burden reduction in *ex vivo* candidiasis infection models in porcine skin, in comparison with conventional cream formulation.

Based on the findings presented in this extensive study, it is shown that the combination approach of NC and dissolving MNs could enhance the penetrability of ITZ in *ex vivo* candidiasis infection models in porcine skin, suggested by the excellent dermatokinetic profiles of ITZ and the great fungal burden decreases. The overriding benefit of this combinatorial delivery system we have shown in this work, compared to cream dosage form and needle-free patches, lead to high residence time specific delivery in the infected skin which could hypothetically improve the efficiency of antifungal therapy in cutaneous candidiasis infection. Based on from these favourable findings, *in vivo* studies must now be carried out in a suitable animal model.

4. Conclusion

Based on the findings presented in this study, it has been shown that the combination approach of NC and dissolving MNs enhanced the penetrability of ITZ in *ex vivo* candidiasis infection models in porcine skin, suggested by the excellent dermatokinetic profiles of ITZ and the great fungal burden decreases. The overriding improvement of the combinatorial delivery system we have shown in this work, led to higher residence time in the skin compared to conventional creams and needle-free patches, which could hypothetically improve the efficiency of antifungal therapy in cutaneous candidiasis. Leading on from these promising results, moving onward, forthcoming studies including *in vivo* efficacy studies must now be conducted to completely investigate the therapeutic efficacy of this approach in animal models of cutaneous candidiasis.

Acknowledgments

The authors wish to thank The Indonesian Endowment Fund for Education (Lembaga Pengelola Dana Pendidikan/LPDP) for supporting this work. This study was also supported in part by Wellcome Trust grant number WT094085MA.

References

[1] F.J. Dowd, Candida albicans infections, Ref. Modul. Biomed. Sci. (2014) 1–3.

[2] L.G. Leanse, X.S. Goh, T. Dai, Quinine improves the fungicidal effects of antimicrobial blue lght: Implications for the treatment of cutaneous candidiasis, Lasers Surg. Med. (2019) 1–7.

[3] J. Delaloye, T. Calandra, Invasive candidiasis as a cause of sepsis in the critically ill patient, Virulence. 5 (2014) 161–169.

[4] T.L. Ray, K.D. Wuepper, Experimental cutaneous candidiasis in rodents, J. Invest. Dermatol. 66 (1976) 29–33.

[5] J. Chandra, D.M. Kuhn, P.K. Mukherjee, L.L. Hoyer, M.A. Ghannoum, Biofilm formation by the fungal pathogen Candida albicans: Development, architecture, and drug resistance, J. Bacteriol. 183 (2001) 5385–5394.

[6] M. Gupta, A.K. Goyal, S.R. Paliwal, R. Paliwal, N. Mishra, B. Vaidya, D. Dube, S.K. Jain, S.P. Vyas, Development and characterization of effective topical liposomal system for localized treatment of cutaneous candidiasis, J. Liposome Res. 20 (2010) 341–350.

[7] A.Y. Zhang, W.L. Camp, B.E. Elewski, Advances in topical and systemic antifungals,

656 Dermatol. Clin. 25 (2007) 165–183.

657 [8] H. Kim, S. Jung, S. Yeo, D. Kim, Y.C. Na, G. Yun, J. Lee, Characteristics of skin
658 deposition of itraconazole solubilized in cream formulation, Pharmaceutics. 11 (2019).

659 [9] M. Boogaerts, J. Maertens, Clinical experience with itraconazole in systemic fungal
660 infections, Drugs. 61 (2001) 39–47.

661 [10] N.R. Patel, K. Damann, C. Leonardi, C.M. Sabliov, Itraconazole-loaded poly(lactic-co-
662 glycolic) acid nanoparticles for improved antifungal activity, Nanomedicine. 5 (2010)
663 1037–1050.

664 [11] A.A. Alhowyan, M.A. Altamimi, M.A. Kalam, A.A. Khan, M. Badran, Z. Binkhathlan,
665 M. Alkholief, A. Alshamsan, Antifungal efficacy of Itraconazole loaded PLGA-
666 nanoparticles stabilized by vitamin-E TPGS: In vitro and ex vivo studies, J. Microbiol.
667 Methods. 161 (2019) 87–95.

668 [12] A.K. Gupta, S. Nolting, Y. De Prost, J. Delescluse, H. Degreef, U. Theissen, R. Wallace,
669 G. Marynissen, P. De Doncker, The use of itraconazole to treat cutaneous fungal
670 infections in children, Dermatology. 199 (1999) 248–252.

671 [13] P. De Doncker, S. Pande, U. Richarz, N. Garodia, Itraconazole: What clinicians should
672 know?, Indian J. Drugs Dermatology. 3 (2017) 4–10.

673 [14] V.B. Clinard, J.D. Smith, Cutaneous fungal infections, US Pharm. 40 (2015) 35–39.

674 [15] P. Berben, R. Mols, J. Brouwers, J. Tack, P. Augustijns, Gastrointestinal behavior of
675 itraconazole in humans – Part 2: The effect of intraluminal dilution on the performance
676 of a cyclodextrin-based solution, Int. J. Pharm. 526 (2017) 235–243.

677 [16] I.S. Mohammad, H. Hu, L. Yin, W. He, Drug nanocrystals: Fabrication methods and
678 promising therapeutic applications, Int. J. Pharm. 562 (2019) 187–202.
679 https://doi.org/10.1016/j.ijpharm.2019.02.045.

680 [17] C.M. Keck, R.H. Müller, Drug nanocrystals of poorly soluble drugs produced by high
681 pressure homogenisation, Eur. J. Pharm. Biopharm. 62 (2006) 3–16.

682 [18] R. Mauludin, R.H. Müller, C.M. Keck, Development of an oral rutin nanocrystal
683 formulation, Int. J. Pharm. 370 (2009) 202–209.

684 [19] R.F. Donnelly, E. Larrañeta, Microarray patches: potentially useful delivery systems for
685 long-acting nanosuspensions, Drug Discov. Today. 23 (2018) 1026–1033.

686 [20] S.M. Pyo, D. Hespeler, C.M. Keck, R.H. Müller, Dermal miconazole nitrate
687 nanocrystals – formulation development, increased antifungal efficacy & skin
688 penetration, Int. J. Pharm. 531 (2017) 350–359.

689 [21] I. Tomić, M. Juretić, M. Jug, I. Pepić, B. Cetina Čižmek, J. Filipović-Grčić, Preparation
690 of in situ hydrogels loaded with azelaic acid nanocrystals and their dermal application
691 performance study, Int. J. Pharm. 563 (2019) 249–258.

692 [22] S. Soisuwan, V. Teeranachaideekul, A. Wongrakpanich, P. Langguth, V.B.

693 Junyaprasert, Impact of uncharged and charged stabilizers on in vitro drug performances
694 of clarithromycin nanocrystals, Eur. J. Pharm. Biopharm. 137 (2019) 68–76.

695 [23] M. Assem, O.M. Khowessah, D. Ghorab, Nano-crystallization as a tool for the
696 enhancement of beclomethasone dipropionate dermal deposition: Formulation, in vitro
697 characterization and ex vivo study, J. Drug Deliv. Sci. Technol. 54 (2019) 101318.

698 [24] A.D. Permana, M.T.C. McCrudden, R.F. Donnelly, Enhanced intradermal delivery of
699 nanosuspensions of antifilariasis drugs using dissolving microneedles: A proof of
700 concept study, Pharmaceutics. 11 (2019) 346.

701 [25] R.F. Donnelly, T.R.R. Singh, D.I.J. Morrow, A.D. Woolfson, Microneedle-mediated
702 transdermal and intradermal drug delivery, in: Wiley-Blackwell, 2012.

703 [26] A.D. Permana, M. Mir, E. Utomo, R.F. Donnelly, Bacterially sensitive nanoparticle-
704 based dissolving microneedles of doxycycline for enhanced treatment of bacterial
705 biofilm skin infection: A proof of concept study, Int. J. Pharm. (2020) 119220.

706 [27] A.D. Permana, I.A. Tekko, M.T.C. McCrudden, Q.K. Anjani, D. Ramadon, H.O.
707 McCarthy, R.F. Donnelly, Solid lipid nanoparticle-based dissolving microneedles: A
708 promising intradermal lymph targeting drug delivery system with potential for enhanced
709 treatment of lymphatic filariasis, J. Control. Release. 316 (2019) 34–52.

710 [28] S. Abdelghany, I.A. Tekko, L. Vora, E. Larrañeta, A.D. Permana, R.F. Donnelly,
711 Nanosuspension-based dissolving microneedle arrays for intradermal delivery of
712 curcumin, Pharmaceutics. 11 (2019) 308.

713 [29] M.T.C. McCrudden, E. Larrañeta, A. Clark, C. Jarrahian, A. Rein-Weston, S. Lachau-
714 Durand, N. Niemeijer, P. Williams, C. Haeck, H.O. McCarthy, D. Zehrung, R.F.
715 Donnelly, Design, formulation and evaluation of novel dissolving microarray patches
716 containing a long-acting rilpivirine nanosuspension, J. Control. Release. 292 (2018)
717 119–129.

718 [30] L.K. Vora, P.R. Vavia, E. Larrañeta, S.E.J. Bell, R.F. Donnelly, Novel nanosuspension-
719 based dissolving microneedle arrays for transdermal delivery of a hydrophobic drug, J.
720 Interdiscip. Nanomedicine. 3 (2018) 89–101.

721 [31] G.B. Romero, C.M. Keck, R.H. Müller, Simple low-cost miniaturization approach for
722 pharmaceutical nanocrystals production, Int. J. Pharm. 501 (2016) 236–244.

723 [32] M. Mir, N. Ahmed, A.D. Permana, A.M. Rodgers, R.F. Donnelly, A.U. Rehman,
724 Enhancement in site-specific delivery of carvacrol against methicillin resistant
725 staphylococcus aureus induced skin infections using enzyme responsive nanoparticles:
726 A proof of concept study, Pharmaceutics. 11 (2019) 606.

727 [33] W.P.M.Z.L.B. Patel J.B., Cockerill R.F., Bradford A.P., Eliopoulos M.G., Hindler A.J.,
728 Jenkins G.S., Lewis S.J., Limbago B., Miller A.L., Nicolau P.D., Pwell M., Swenson
729 M.J., Traczewski M.M., Turnidge J.D., Methods for Dilution Antimicrobial
730 Susceptibility Tests for Bacteria That Grow Aerobically; Approved Standard—Tenth
731 Edition., CLSI (Clinical Lab. Stand. Institute). 35 (2015).

732 [34] M. Mir, A.D. Permana, N. Ahmed, G.M. Khan, A. ur Rehman, R.F. Donnelly,

Enhancement in site-specific delivery of carvacrol for potential treatment of infected wounds using infection responsive nanoparticles loaded into dissolving microneedles: A proof of concept study, Eur. J. Pharm. Biopharm. 147 (2020) 57–68.

[35] H. Chen, L. Li, Y. Liu, M. Wu, S. Xu, G. Zhang, C. Qi, Y. Du, M. Wang, J. Li, X. Huang, In vitro activity and post-antibiotic effects of linezolid in combination with fosfomycin against clinical isolates of Staphylococcus aureus, Infect. Drug Resist. 11 (2018) 2107–2115.

[36] P. González-Vázquez, E. Larrañeta, M.T.C. McCrudden, C. Jarrahian, A. Rein-Weston, M. Quintanar-Solares, D. Zehrung, H. McCarthy, A.J. Courtenay, R.F. Donnelly, Transdermal delivery of gentamicin using dissolving microneedle arrays for potential treatment of neonatal sepsis, J. Control. Release. 265 (2017) 30–40.

[37] E. Larrañeta, J. Moore, E.M. Vicente-Pérez, P. González-Vázquez, R. Lutton, A.D. Woolfson, R.F. Donnelly, A proposed model membrane and test method for microneedle insertion studies, Int. J. Pharm. 472 (2014) 65–73.

[38] Y. Zhang, M. Huo, J. Zhou, S. Xie, PKSolver: An add-in program for pharmacokinetic and pharmacodynamic data analysis in Microsoft Excel, Comput. Methods Programs Biomed. 99 (2010) 306–314.

[39] A.D. Permana, M. Mir, E. Utomo, R.F. Donnelly, Bacterially sensitive nanoparticle-based dissolving microneedles of doxycycline for enhanced treatment of bacterial biofilm skin infection: A proof of concept study, Int. J. Pharm. (2020) 119220.

[40] C.M. Keck, R.H. Müller, Size analysis of submicron particles by laser diffractometry--90% of the published measurements are false., Int. J. Pharm. 355 (2008) 150–63.

[41] S.L. Levit, R.M. Stwodah, C. Tang, Rapid, room temperature nanoparticle drying and low-energy reconstitution via electrospinning, J. Pharm. Sci. 107 (2018) 807–813.

[42] A.J. Paredes, J.M. Llabot, S. Sánchez Bruni, D. Allemandi, S.D. Palma, Self-dispersible nanocrystals of albendazole produced by high pressure homogenization and spray-drying, Drug Dev. Ind. Pharm. 42 (2016) 1564–1570.

[43] A.D. Permana, R.N. Utami, A.J. Courtenay, M.A. Manggau, R.F. Donnelly, L. Rahman, Phytosomal nanocarriers as platforms for improved delivery of natural antioxidant and photoprotective compounds in propolis: An approach for enhanced both dissolution behaviour in biorelevant media and skin retention profiles, J. Photochem. Photobiol. B Biol. 205 (2020) 111846.

[44] S. Dash, P.N. Murthy, L. Nath, P. Chowdhury, Kinetic modelling on drug release from controlled drug delivery systems, Acta Pol. Pharm. - Drug Res. 67 (2010) 217–223.

[45] T. Niwa, Y. Imagawa, H. Yamazaki, Drug interactions between nine antifungal agents and drugs metabolized by human Cytochromes P450, Curr. Drug Metab. 15 (2014) 651–679.

[46] C.H.W. Koks, P.L. Meenhorst, A. Bult, J.H. Beijnen, Itraconazole solution: Summary of pharmacokinetic features and review of activity in the treatment of fluconazole-resistant oral candidosis in HIV-infected persons, Pharmacol. Res. 46 (2002) 195–201.

[47] W.J. Steinbach, D.A. Stevens, Review of newer antifungal and immunomodulatory strategies for invasive aspergillosis, Clin. Infect. Dis. 37 (2003) S157-87.

[48] M. Tato, Y. López, M.I. Morosini, A. Moreno-Bofarull, F. Garcia-Alonso, D. Gargallo-Viola, J. Vila, R. Cantón, Characterization of variables that may influence ozenoxacin in susceptibility testing, including MIC and MBC values, Diagn. Microbiol. Infect. Dis. 78 (2014) 263–267.

[49] M.T.C. McCrudden, A.Z. Alkilani, C.M. McCrudden, E. McAlister, H.O. McCarthy, A.D. Woolfson, R.F. Donnelly, Design and physicochemical characterisation of novel dissolving polymeric microneedle arrays for transdermal delivery of high dose, low molecular weight drugs, J. Control. Release. 180 (2014) 71–80.

[50] R.F. Donnelly, K. Moffat, A.Z. Alkilani, E.M. Vicente-Pérez, J. Barry, M.T.C. McCrudden, A.D. Woolfson, Hydrogel-forming microneedle arrays can be effectively inserted in skin by self-application : A pilot study centred on pharmacist intervention and a patient information leaflet, Pharm. Res. 31 (2014) 1989–1999.

[51] R.F. Donnelly, M.J. Garland, D.I.J. Morrow, K. Migalska, T. Raghu, R. Singh, R. Majithiya, A.D. Woolfson, Optical coherence tomography is a valuable tool in the study of the effects of microneedle geometry on skin penetration characteristics and in-skin dissolution, J. Control. Release. 147 (2010) 333–341.

[52] R.E.M. Lutton, E. Larrañeta, M.C. Kearney, P. Boyd, A.D. Woolfson, R.F. Donnelly, A novel scalable manufacturing process for the production of hydrogel-forming microneedle arrays, Int. J. Pharm. 494 (2015) 417–429.

BUKTI ACCEPTED

Universitas Hasanuddin

Andi Dian Permana <andi.dian.permana@farmasi.unhas.ac.id>

Fwd: Decision on submission to European Journal of Pharmaceutics and Biopharmaceutics

1 message

Andi Permana <apermana01@qub.ac.uk> Tue, Apr 4, 2023 at 4:21 PM
To: Andi Dian Permana <andi.dian.permana@farmasi.unhas.ac.id>

Get Outlook for iOS

From: Ryan Donnelly <R.Donnelly@qub.ac.uk>
Sent: Monday, June 29, 2020 3:56:48 PM
To: Andi Permana <apermana01@qub.ac.uk>
Cc: Alejandro Paredes <A.Paredes@qub.ac.uk>
Subject: Fw: Decision on submission to European Journal of Pharmaceutics and Biopharmaceutics

Brilliant!

Congratulations Dian!

Ryan

Professor Ryan F. Donnelly
Chair in Pharmaceutical Technology
School of Pharmacy
Queen's University Belfast
Medical Biology Centre
97 Lisburn Road
Belfast
BT9 7BL
UK
Tel: +44 (0) 2890 972 251
Fax: +44 (0) 2890 247 794
Email: r.donnelly@qub.ac.uk

From: em.ejpb.0.6c461b.bab2b6a3@editorialmanager.com <em.ejpb.0.6c461b.bab2b6a3@editorialmanager.com> on behalf of European Journal of Pharmaceutics and Biopharmaceutics <em@editorialmanager.com>
Sent: 29 June 2020 06:25
To: Ryan Donnelly <R.Donnelly@qub.ac.uk>
Subject: Decision on submission to European Journal of Pharmaceutics and Biopharmaceutics

Manuscript Number: EJPB-D-20-00409R1

Dissolving Microneedle-Mediated Dermal Delivery of Itraconazole Nanocrystals for Improved Treatment of Cutaneous Candidiasis

Dear Professor Donnelly,

Thank you for submitting your manuscript to European Journal of Pharmaceutics and Biopharmaceutics.

I am pleased to inform you that your manuscript has been accepted for publication.

My comments, and any reviewer comments, are below.
Your accepted manuscript will now be transferred to our production department. We will create a proof which you will be asked to check, and you will also be asked to complete a number of online forms required for publication. If we need additional information from you during the production process, we will contact you directly.

We appreciate you submitting your manuscript to European Journal of Pharmaceutics and Biopharmaceutics and hope you will consider us again for future submissions.

Kind regards,
Thomas Rades
Editor

European Journal of Pharmaceutics and Biopharmaceutics

Editor and Reviewer comments:

More information and support

FAQ: When and how will I receive the proofs of my article?
https://service.elsevier.com/app/answers/detail/a_id/6007/p/10592/supporthub/publishing/related/

You will find information relevant for you as an author on Elsevier's Author Hub: https://www.elsevier.com/authors

FAQ: How can I reset a forgotten password?
https://service.elsevier.com/app/answers/detail/a_id/28452/supporthub/publishing/kw/editorial+manager/

For further assistance, please visit our customer service site: https://service.elsevier.com/app/home/supporthub/publishing/. Here you can search for solutions on a range of topics, find answers to frequently asked questions, and learn more about Editorial Manager via interactive tutorials. You can also talk 24/7 to our customer support team by phone and 24/7 by live chat and email.
